AGU PUBLICATIONS

Geophysical Research Letters

RESEARCH LETTER
10.1002/2017GL072975

Key Points:
- Sea-to-air fluxes of dimethyl sulfide were observed to be factor of 10 larger than either isoprene or monoterpenes over the North Atlantic Ocean during fall
- The production rate of secondary organic aerosol, stemming from marine isoprene and monoterpene emission, is calculated to be small compared to primary emissions
- Rare, intense ocean emission of monoterpenes can have a sizeable impact on particle size distributions and in turn the number concentration of cloud condensation nuclei

Supporting Information:
- Supporting Information S1

Correspondence to:
T. H. Bertram,
timothy.bertram@wisc.edu

Citation:
Kim, M. J., G. A. Novak, M. C. Zoerb, M. Yang, B. W. Blomquist, B. J. Huebert, C. D. Cappa, and T. H. Bertram (2017), Air-Sea exchange of biogenic volatile organic compounds and the impact on aerosol particle size distributions, *Geophys. Res. Lett.*, *44*, 3887–3896, doi:10.1002/2017GL072975.

Received 6 FEB 2017
Accepted 10 APR 2017
Accepted article online 12 APR 2017
Published online 24 APR 2017

Air-Sea exchange of biogenic volatile organic compounds and the impact on aerosol particle size distributions

Michelle J. Kim[1,2], Gordon A. Novak[3], Matthew C. Zoerb[4,5], Mingxi Yang[6], Byron W. Blomquist[7], Barry J. Huebert[8], Christopher D. Cappa[9], and Timothy H. Bertram[3]

[1]Scripps Institution of Oceanography, University of California, San Diego, La Jolla, California, USA, [2]Now at Division of Geological and Planetary Sciences, California Institute of Technology, Pasadena, California, USA, [3]Department of Chemistry, University of Wisconsin-Madison, Madison, Wisconsin, USA, [4]Department of Chemistry and Biochemistry, University of California, San Diego, La Jolla, California, USA, [5]Now at Department of Chemistry and Biochemistry, California Polytechnic State University, San Luis Obispo, California, USA, [6]Plymouth Marine Laboratory, Plymouth, UK, [7]Cooperative Institute for Research in Environmental Sciences, University of Colorado Boulder, Boulder, Colorado, USA, [8]School of Ocean and Earth Sciences and Technology, University of Hawai'i at Mānoa, Honolulu, Hawaii, USA, [9]Department of Civil and Environmental Engineering, University of California, Davis, California, USA

Abstract We report simultaneous, underway eddy covariance measurements of the vertical flux of isoprene, total monoterpenes, and dimethyl sulfide (DMS) over the Northern Atlantic Ocean during fall. Mean isoprene and monoterpene sea-to-air vertical fluxes were significantly lower than mean DMS fluxes. While rare, intense monoterpene sea-to-air fluxes were observed, coincident with elevated monoterpene mixing ratios. A statistically significant correlation between isoprene vertical flux and short wave radiation was not observed, suggesting that photochemical processes in the surface microlayer did not enhance isoprene emissions in this study region. Calculations of secondary organic aerosol production rates (P_{SOA}) for mean isoprene and monoterpene emission rates sampled here indicate that P_{SOA} is on average <0.1 μg m^{-3} d^{-1}. Despite modest P_{SOA}, low particle number concentrations permit a sizable role for condensational growth of monoterpene oxidation products in altering particle size distributions and the concentration of cloud condensation nuclei during episodic monoterpene emission events from the ocean.

1. Background

Biogenic volatile organic compounds (BVOCs), primarily emitted from photosynthetic organisms, play a controlling role in both regulating oxidant loadings [*Houweling et al.*, 1998; *Taraborrelli et al.*, 2012] and setting the production rate of secondary organic aerosol (SOA) in remote environments [*Griffin et al.*, 1999; *Hoffmann et al.*, 1997]. To date, the vast majority of research has focused on terrestrial sources of BVOC, with specific attention to the factors that control emissions of isoprene (C_5H_8), monoterpenes ($C_{10}H_{16}$), and sesquiterpenes ($C_{15}H_{24}$). Global terrestrial emissions of isoprene, the most abundant BVOC, have been estimated to be between 500 and 750 Tg C yr^{-1} [*Guenther et al.*, 2006]. Emission rates of monoterpenes and sesquiterpenes are estimated to be considerably smaller but can have a disproportionate impact on aerosol production rates due to their higher SOA yields [e.g., *Griffin et al.*, 1999] and ability to produce extremely low volatility oxidation products [*Ehn et al.*, 2014]. Global marine isoprene emissions are estimated to be between 0.1 and 12 Tg C yr^{-1} [*Arnold et al.*, 2009; *Gantt et al.*, 2010; *Luo and Yu*, 2010; *Meskhidze et al.*, 2009; *Palmer and Shaw*, 2005]. Even less is known about marine monoterpene emissions, with the sole estimate bracketing the global flux between 0.01 and 29.5 Tg C yr^{-1} [*Luo and Yu*, 2010]. For comparison, the global, annual sea-to-air flux of dimethyl sulfide (DMS) is estimated to be 14.7–21.1 Tg C yr^{-1} [*Kloster et al.*, 2006; *Lana et al.*, 2011; *Land et al.*, 2014]. Similar to terrestrial emissions, the spatiotemporal distribution of marine BVOC emissions is highly variable, depending strongly on the abundance and species of photosynthetic organism [*Shaw et al.*, 2010] coupled to nutrient availability [*Zindler et al.*, 2014].

Despite comparatively lower average emission rates, it has been suggested that marine BVOC emissions in highly biologically active regions of the oceans can (1) impact oxidant loadings in the marine boundary layer (MBL) [*Donahue and Prinn*, 1990; *Mihalopoulos et al.*, 2007; *Palmer and Shaw*, 2005], (2) contribute to SOA production [*Arnold et al.*, 2009; *Gantt et al.*, 2010], and (3) alter particle size and microphysical properties, thus impacting cloud formation and persistence in the MBL [*Kruger and Grassl*, 2011; *Meskhidze and Nenes*, 2006]. To date, the majority of marine VOC research has focused on linkages between marine emissions of

DMS and low-level clouds [*Charlson et al*., 1987, 1989; *Quinn and Bates*, 2011], with comparatively less work focused on isoprene and monoterpene emissions and their subsequent impact on oxidant levels, aerosol particle number and size distributions, and cloud formation mechanisms.

Laboratory monoculture studies have demonstrated that marine phytoplankton can efficiently produce both isoprene and select monoterpenes, with production rates dependent on phytoplankton speciation, ambient conditions, and nutrient loadings [*Shaw et al*., 2010]. *Ciuraru et al.* [2015] suggested that isoprene can also be produced photochemically in the sea surface microlayer (SSML) and emitted to the atmosphere following the excitation of dissolved organic matter found in the presence of surfactant films. Surface seawater isoprene concentrations have been reported in the range of 0.1–100 pmol L^{-1}, with higher concentrations often, but not always, correlated with chlorophyll *a* [*Shaw et al*., 2010]. *Zindler et al.* [2014] report a mean isoprene surface seawater concentration of 25.7 ± 14.7 pmol L^{-1} for an Atlantic Ocean transect between Germany and South Africa, with peak isoprene seawater concentrations (>100 pmol L^{-1}) associated with nutrient availability and no relationship to chlorophyll *a*. Gas-phase isoprene mixing ratios, sampled at the ocean surface from research vessels, have been observed as high as 375 ppt during bloom conditions (chlorophyll *a* = 1 mg m^{-3}) [*Yassaa et al*., 2008]. Under nonbloom conditions, gas-phase isoprene mixing ratios are routinely less than 20 ppt [*Shaw et al.,* 2010], a function of both spatially variable production rates and a short atmospheric lifetime. *Meskhidze et al.* [2015] reported that per-cell monoterpene production rates were an order of magnitude smaller than isoprene production, with monoterpenes often dominated by α-pinene (>70%), suggesting that seawater and gas-phase monoterpene concentrations should be smaller than isoprene, although there are a paucity of monoterpene surface seawater and gas-phase measurements in the MBL. *Yassaa et al*., 2008 presented the most complete underway monoterpene data set, reporting average MBL gas-phase monoterpene mixing ratios of 125 ppt (bloom) and 5 ppt (nonbloom) in the southern Atlantic Ocean.

To assess the impact of marine BVOC on atmospheric oxidation and aerosol particle size distributions in box, regional, or global chemistry models, estimates of BVOC vertical fluxes are required. To date, the flux (*F*) of BVOCs across the air-ocean interface has not been measured directly, only calculated from measurements of surface seawater (C_w) and gas-phase (C_a) concentrations and estimates of the total transfer velocity (K_t),

$$F = K_t\left(C_w - \frac{C_a}{\alpha}\right) \tag{1}$$

where α is the dimensionless liquid over gas solubility. Estimates of isoprene fluxes based on concentration differences range between 0.1 and 21 × 10^7 molecules cm^{-2} s^{-1} [*Broadgate et al*., 1997; *Matsunaga et al*., 2002]. *Ciuraru et al.* [2015] suggested that photosensitized isoprene production could lead to fluxes as large as 0.8–1.7 × 10^9 molecules cm^{-2} s^{-1}, estimated for irradiated SML samples accounting for surface enrichment. Photochemical production of isoprene at the interface would lead to strong seawater concentration gradients that complicate the interpretation of E1 as measurements of C_w are often taken at depths of 5 m. Unlike isoprene, the lack of existing surface seawater measurements of monoterpenes prohibits calculation of monoterpene fluxes via E1 and global estimates of monoterpene emissions are scaled from laboratory monoculture experiments or inferred from select monoterpene gas-phase mixing ratios [*Luo and Yu*, 2010].

Indirect evidence for marine BVOC emissions and subsequent photochemical processing has been shown in aerosol composition measurements. *Hu et al.* [2013] analyzed SOA tracers, finding that isoprene- and monoterpene-derived SOA concentrations were as large as 95 and 11 ng m^{-3} (respectively) in regions of phytoplankton blooms. In that study isoprene SOA tracers were on average 14 ± 11 ng m^{-3} in the Northern Hemisphere and less than 10 ng m^{-3} in the Southern Hemisphere, while monoterpene SOA tracers were on average less than 10 ng m^{-3} in both the Northern and Southern Hemispheres. *Hu et al.* [2013] also found that monoterpene SOA tracers exceeded isoprene SOA tracers in North Atlantic samples.

Here we present concurrent isoprene, total monoterpene, and DMS gas-phase mixing ratio and vertical flux measurements made aboard the R/V *Knorr* during the High Wind Gas Exchange Study (HiWinGS) in the North Atlantic Ocean during fall 2013 [*Yang et al*., 2014]. To our knowledge, this work represents the first direct measurements of marine isoprene and monoterpene sea-to-air fluxes. The observations are used to constrain the impact of BVOC emissions on particle size distributions and ultimately the concentration of cloud condensation nuclei (CCN).

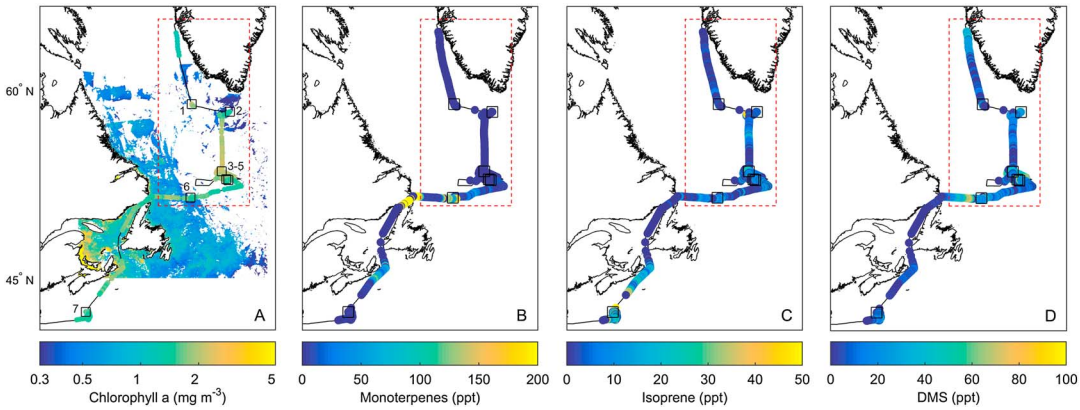

Figure 1. (a) Satellite measurement of chlorophyll *a* averaged over the 2013 High Wind Gas Exchange Study (HiWinGS) sampling period, courtesy of NEODAAS. Underway measurements of chlorophyll *a* are shown along the cruise track using the same color scale. Underway measurements of gas-phase mixing ratios (color scale, ppt) of (b) monoterpenes, (c) isoprene, and (d) dimethyl sulfide (DMS). Trace gas mixing ratios in the boxed region are considered to be dominated by air-sea exchange.

2. Underway Measurements of Marine BVOC Mixing Ratios and Vertical Flux

The HiWinGS cruise traversed from Nuuk, Greenland, to Woods Hole, MA, during October and November 2013 (Figure 1). The primary objective of HiWinGS was investigation of the physical processes that control air-sea gas exchange during high wind conditions. High wind speeds were encountered during HiWinGS (up to 25 m s^{-1} hourly average at 10 m), not atypical of the sampling domain. Underway measurements of surface chlorophyll *a* in the sampling region during October and November 2013 were on average 1.59 mg m^{-3} (Figure 1a). DMS, isoprene, and sum monoterpenes mixing ratios (C_a) were measured using benzene cluster cation chemical ionization time-of-flight mass spectrometry (CI-ToFMS) [*Bertram et al.*, 2011; *Kim et al.*, 2016]. Air-sea vertical fluxes (F) were determined via the eddy covariance method, where 5–10 Hz measurements of mixing ratios were correlated with motion-corrected vertical wind velocity (w) to compute F as

$$F = \overline{w' C_a'} \tag{2}$$

where C_a' and w' represent the deviation of C_a and w from the mean value and the overbar denotes an average over an interval, here ~45–60 min. A more detailed discussion of the methodology can be found in the supporting information [*Bariteau et al.*, 2010; *Blomquist et al.*, 2006; *McGillis et al.*, 2001; *Spirig et al.*, 2005]. DMS vertical fluxes were made from two independent sampling systems. The first was the University of Hawaii's atmospheric pressure ionization mass spectrometer with an isotopically labeled standard [*Blomquist et al.*, 2010]. The second was the CI-ToFMS, which also measured isoprene and total monoterpene vertical fluxes [*Kim et al.*, 2016]. We showed previously that DMS mixing ratio measurements from the two instruments were in strong agreement ($R^2 > 0.95$) [*Kim et al.*, 2016]. Here (Figure S3) we show that DMS vertical flux measurements from the two instruments are also in strong agreement (slope = 1.01, intercept = 8.9×10^7 molecules cm^{-2} s^{-1}, $R^2 = 0.7$). The time series of DMS, isoprene, and total monoterpene vertical flux measurements for HiWinGS are shown in Figures 2a–2c.

Gas-phase mixing ratios for DMS, isoprene, and total monoterpenes are shown along the HiWinGS cruise track in Figures 1b–1d, and campaign-wide statistics are listed in Table S1 in the supporting information. For the boxed regions in Figure 1, considered to be dominated by air-sea exchange, we observe a mean DMS mixing ratio of 35.3 ± 22.3 ppt, with a median of 28.2 ppt. The mean isoprene mixing ratio in the same region was 10.3 ± 6.5 ppt, with a median of 9.98 ppt. The mean total monoterpene mixing ratio was 17.1 ± 34 ppt, with a median of 3.2 ppt. The strong divergence between the mean and median monoterpene mixing ratios highlights that the monoterpene distribution is not normally distributed and that episodic, high monoterpene emissions distort the mean. One such event is shown in the open ocean boxed region centered at 52°N, 50°W, where total monoterpene emissions peak near 100 ppt. Periods of elevated monoterpene

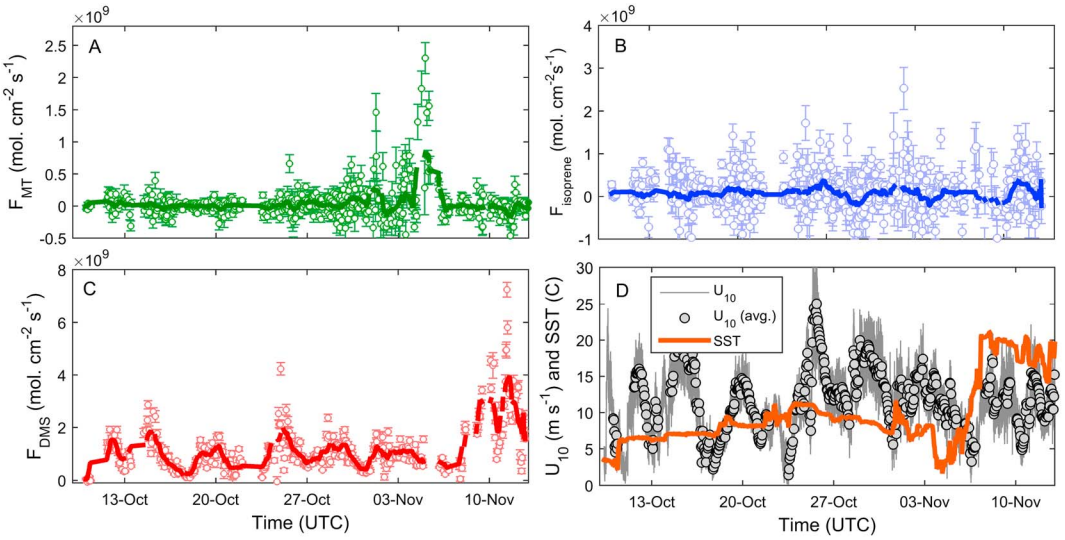

Figure 2. Time series of sea-to-air vertical flux of (a) monoterpenes, (b) isoprene, and (c) dimethyl sulfide (DMS) in units of molecules cm^{-2} s^{-1}. The solid colored line represents a 6 h running mean of the measurements. (d) Wind speed (U_{10}, m s^{-1}) and sea surface temperature (SST, °C) are shown.

fluxes occurred following two marked changes in sea state: (1) a deepening of the mixed layer on 25 October after a storm (>25 m s^{-1} winds) as evidenced by temperature profiles from daily conductivity-temperature-depth casts and (2) a frontal passage into the Labrador Current marked by a large decrease in sea surface temperature (Figure 2). Both suggest recent vertical mixing, which can be driven by large wave breaking from very strong winds or processes such as coastal upwelling. This can lead to nutrient replenishment in the euphotic layer and spur microorganism growth. Monoterpene emissions from 1.2×10^8 to 6.6×10^8 molecules cm^{-2} s^{-1}, and peak emissions for the cruise were observed in coastal areas influenced by the Labrador Current. From the available measurements, we suggest a potential mechanism where nutrient-limited microorganisms in the sea surface drove monoterpene production, resulting in enhanced monoterpene seawater concentrations and sea-to-air emission after vertical mixing. Nutrient-limited microorganisms, such as diatoms, are commonly found in the region during other parts of the year [*Fragoso et al.*, 2016]. However, nutrient control of monoterpene-producing biology in this region cannot be confirmed without in situ sampling of the water column. Alternative mechanisms including the direct transport of monoterpenes to the surface layer by vertical mixing or nutrient-enhanced production of monoterpenes by robust microorganisms (e.g., dinoflagellates) would also be consistent with these observations.

Backward trajectory analysis (Figure S1) indicates that the air last passed over land (Newfoundland, CA) 9 h prior to sampling [*Stein et al.*, 2015], which is approximately one *e*-fold in α-pinene at diel average O_3 mixing ratios of 20 ppb and OH concentrations of 2.5×10^5 molecules cm^{-3}. In comparison, the eddy covariance flux footprint was typically less than 2 km, suggesting that flux measurements made during HiWinGS were not influenced by terrestrial emissions. This highlights both the challenges of interpreting concentration data in the context of ocean emissions and the unique constraints that underway flux measurements can provide for source apportionment and establishing global emissions estimates.

Isoprene and monoterpene sea-to-air vertical fluxes were small, with campaign averages of 5.0×10^7 and 2.63×10^7 molecules cm^{-2} s^{-1} (or 71.8 and 37.7 nmol d^{-1} m^{-2}), respectively, significantly lower than the mean DMS flux (1.04×10^9 molecules cm^{-2} s^{-1} or 1.50×10^3 nmol day^{-1} m^{-2}). Isoprene fluxes observed during HiWinGS are consistent with previous indirect measurements, which range between 0.1 and 21×10^7 molecules cm^{-2} s^{-1} [*Broadgate et al.*, 1997; *Matsunaga et al.*, 2002] and global models [*Booge et al.*, 2016]. Based on wind conditions of HiWinGS (mean speed 11 m s^{-1}) and mean observed isoprene mixing ratios (10.3 ± 6.5 ppt), the mean isoprene flux translates to an effective waterside concentration of 21 pmol L^{-1} using the gas transfer parameterization of *Johnson* [2010] and the water-phase transfer

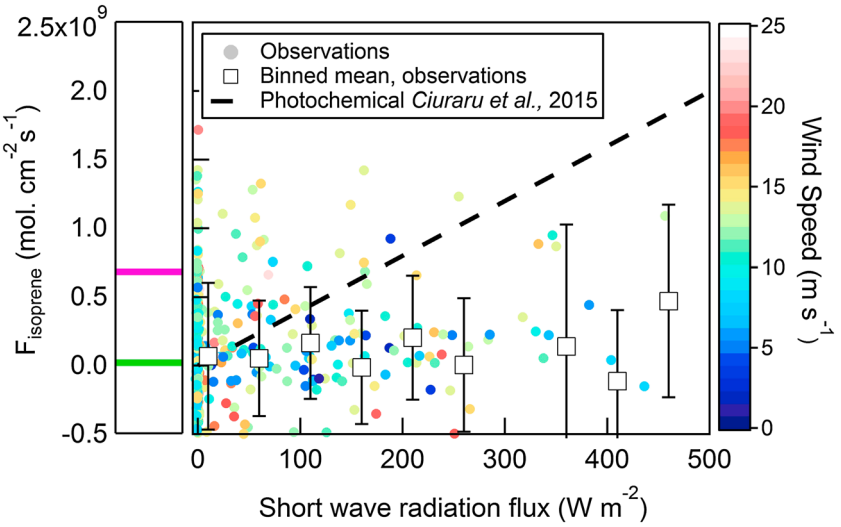

Figure 3. Underway eddy covariance flux measurements of isoprene sea-to-air exchange as a function of short wave radiation flux (black squares, binned means with standard deviation). Individual measurements are shown colored by wind speed (U_{10}, m s^{-1}). Prior field-based determinations of isoprene sea-to-air fluxes in the North Sea and Northeast Pacific [*Broadgate et al*., 1997] and at Mace Head [*Broadgate et al*., 2004] are shown with green and pink lines, respectively. Laboratory determination of photochemical isoprene production from sea surface microlayer samples, as determined by *Ciuraru et al.* [2015], is also shown with the black dashed line (for ER = 1) linearly scaled to short wave radiation fluxes (e.g., $F_{isoprene}$ = 8.0 × 10^8 molecules cm^{-2} s^{-1} at SWR = 200 W m^{-2}.

velocity parameterization of *Nightingale et al.* [2000]. To sustain the observed gas-phase mixing ratios, the calculated effective waterside concentration is within the range of previous field measurements (0.1–100 pmol L^{-1}) [*Shaw et al*., 2010].

Despite the late fall observation period for HiWinGS (October–November), there was sufficient variability in short wave radiation (SWR) to determine if the observed isoprene flux correlates with SWR flux, which would be expected if photochemical production were dominant. As shown in Figure 3, isoprene vertical flux appears independent of SWR flux. Isoprene emission rates measured from irradiated sea surface microlayer samples, in the laboratory [*Ciuraru et al*., 2015], having been doped with photosensitizers, corrected for surface enrichment (SE = 1) and linearly scaled to SWR, suggest much larger emission fluxes (8.0 × 10^8 molecules cm^{-2} s^{-1} at SWR = 200 W m^{-2}) than observed here (blue dashed line) [*Ciuraru et al*., 2015]. Also shown in Figure 3 are the prior estimates of isoprene emission fluxes taken from the North Sea measurements of *Broadgate et al.* [1997] and studies of *Broadgate et al.* [2004] at Mace Head. In our study, a dependence of vertical flux on SWR was not observed for either DMS or total monoterpenes. While the results of this study do not support photochemical isoprene production, future field and laboratory-based studies are warranted, particularly in more biologically active waters.

Due to the absence of seawater monoterpene concentration measurements in the literature and a paucity of gas-phase mixing ratio measurements, there is little framework for comparison of our monoterpene flux determinations. The mean monoterpene flux during the open ocean segments of HiWinGS (boxed region in Figure 1) was 2.63 × 10^7 molecules cm^{-2} s^{-1}. This flux suggests an effective mean waterside concentration of monoterpenes of 13 pmol L^{-1} using the gas transfer parameterization of *Johnson* [2010] and mean HiWinGS wind and median monoterpene gas-phase mixing ratios. Variability in sea-to-air fluxes should be coincident with monoterpene mixing ratios in time due to their short atmospheric lifetimes, ranging between 1 and 5 h for different isomers. We calculate the steady state monoterpene concentration associated with a prescribed sea-to-air flux using a time-dependent box model that couples ocean emission with photochemical oxidation (Text S1). The relationship between monoterpene sea-to-air flux and MBL mixing ratios can be established for given O_3 and OH concentrations and MBL height. This relationship is shown alongside the set of observations from HiWinGS in Figure S4. The observations demonstrate a clear relationship between vertical flux and concentration as suggested by the model analyses (blue line, $[O_3]$ = 20 ppb, $[OH]_{24h}$ = 2.5 × 10^5 molecules cm^{-3},

MBL = 600 m). However, the bulk of the observations fall above the blue line suggesting (1) that contributions from nonoceanic sources may be significant, (2) a breakdown in the approximation that instantaneous concentration and flux measurements are constant for multiple monoterpene lifetimes, and/or (3) a higher contribution of lower reactivity monoterpenes (e.g., camphene compared to α-pinene) to the total monoterpene signal. For comparison, the sustained monoterpene mixing ratios of 125 and 5 ppt, as observed by *Yassaa et al.* [2008] in the Southern Ocean during in and out of bloom conditions, would require fluxes greater than 1.0×10^{10} molecules cm^{-2} s^{-1} and 5×10^{8} molecules cm^{-2} s^{-1}, respectively, for $[O_3]$ = 20 ppb, $[OH]_{24h} = 2.5 \times 10^{5}$ molecules cm^{-3}, MBL = 600 m [*Kawai et al.*, 2015], comparable to that required in this study.

To provide an approximate comparison of our observations with existing global measurements, we simply scale our mean fluxes to global ocean surface area. This yields global, annual mean sea-to-air fluxes of 4.71, 0.57, and 0.60 Tg C yr^{-1} for DMS, isoprene, and monoterpenes, respectively. Compared to global biogeochemical model outputs, our surface area-scaled estimate of DMS sea-to-air fluxes is approximately 3–5 times smaller than literature estimates [*Kloster et al.*, 2006; *Lana et al.*, 2011; *Land et al.*, 2014]. As expected, this highlights the fact that the conditions during the HiWinGS campaign (e.g., marine winds, biological activity, and speciation) may not be fully representative of global average conditions. A comparable offset between HiWinGS measurements and global models for BVOC emissions may not apply, as BVOC production has been shown to be driven by different species and physical conditions in both laboratory tests and in in situ measurements [*Meskhidze et al.*, 2015; *Zindler et al.*, 2014]. Nonetheless, the exercise provides a needed constraint on the magnitude of existing estimates of isoprene (0.1–12 Tg C yr^{-1}) and monoterpene (0.01–29.5 Tg C yr^{-1}) global, annual flux, suggesting that BVOC fluxes are on the lower end of the previous estimates.

3. Impact of Marine Secondary Organic Aerosol Production on Cloud Condensation Nuclei

Isoprene and monoterpene oxidation products have been observed previously in marine organic aerosol, contributing upward of 100 ng m^{-3} in regions of intense phytoplankton blooms and averaging 17 ng m^{-3} in one study [*Hu et al.*, 2013]. Here we use average and episodic BVOC fluxes measured during HiWinGS to estimate a range in SOA production rates, based on prior determinations of SOA yields in low NO_x and low organic aerosol mass regimes. Organic aerosol (OA) mass concentrations were not measured on HiWinGS; however, prior measurements of OA in remote marine environments suggest that OA mass concentrations are typically less than 0.5 μg m^{-3} [*Russell et al.*, 2010]. SOA yields from isoprene photoxidation under such OA concentrations are thought to be very low [*Carlton et al.*, 2009]; however, new chamber measurements suggest that SOA mass yield could reach 0.15 under select conditions [*Liu et al.*, 2016]. SOA production from the ozonolysis of monoterpenes [*Ehn et al.*, 2014; *Jokinen et al.*, 2015], and most recently OH reactions with monoterpenes [*Berndt et al.*, 2016], has been shown to generate prompt, extremely low volatility organic compounds (ELVOCs) with relatively high yield for OA concentrations that might be more typical of the marine environment.

SOA production rates (P_{SOA}) were calculated using a time-dependent photochemical box model, as a function of isoprene and monoterpene sea-to-air fluxes, isomer-averaged monoterpene ELVOC yields, and isoprene SOA yields (Text S1). In the model, monoterpenes are emitted from the surface ocean and oxidized by OH and O_3, forming ELVOC at the prescribed yield. ELVOCs are then permitted to irreversibly partition to the aerosol phase at the gas-aerosol collision limit, which is reasonable for such low-volatility compounds. P_{SOA} is shown as a function of the assumed ELVOC yield and the monoterpene flux in Figure 4a for the model case of O_3 = 20 ppb, OH = 2.5×10^{5} molecules cm^{-3}, N_p = 100 cm^{-3}, d_p (dry, geometric mean) = 180 nm, and a marine boundary layer height of 600 m [*Kawai et al.*, 2015]. For example, using an ELVOC yield of 0.05, P_{SOA} is calculated to be 0.2 ng m^{-3} d^{-1} and 25 ng m^{-3} d^{-1} for mean and maximum monoterpene fluxes observed during HiWinGS. Isoprene SOA production was also assessed in the model under two yield approximations (0.025 and 0.15). For low isoprene yield conditions (Y = 0.025), P_{SOA} derived from isoprene was calculated to be 0.1 ng m^{-3} d^{-1} and 2 ng m^{-3} d^{-1} for mean and maximum isoprene fluxes observed in this study. For high isoprene yield conditions (Y = 0.15), P_{SOA} derived from isoprene was calculated to be 0.7 ng m^{-3} d^{-1} and 12.5 ng m^{-3} d^{-1} for mean and maximum isoprene fluxes observed during HiWinGS. Assuming

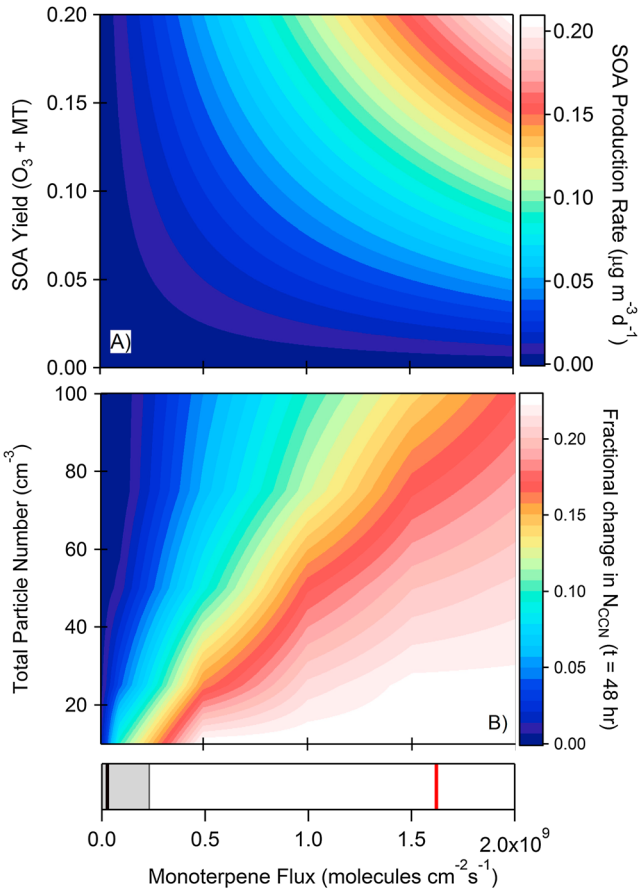

Figure 4. (a) Modeled secondary organic aerosol (SOA) production rate as a function of monoterpene air-sea exchange and condensable product yield. (b) Modeled change in cloud condensation number due to condensational growth after 48 h as a function of monoterpene flux and total particle number concentrations (SS = 0.1%, Y_{SOA} = 0.05). The bottom panel shows the mean (black line), standard deviation (gray shaded region) and maximum (red) monoterpene flux during HiWinGS. SOA production rates were computed using $[OH]_{24h} = 2.5 \times 10^5$ molecules cm^{-3}, $[O_3]$ = 20 ppb, and boundary layer height of 600 m.

an average particle lifetime of 10 days with respect to dry deposition [*Slinn and Slinn*, 1980], low-volatility isoprene and monoterpene oxidation products are likely not to exceed 10 ng m^{-3} outside of bloom conditions, consistent with the observations of *Hu et al.* [2013].

Despite small P_{SOA} relative to terrestrial environments, low particle number concentrations characteristic of marine environments (N_p ~ 100 cm^{-3}) may permit modest P_{SOA} to have an outsized impact on the shape of the particle size distributions and, in turn, cloud condensation number concentrations (N_{CCN}). To assess the extent to which marine SOA, derived from BVOC sea-to-air emissions and subsequent oxidation, may impact particle size distributions, we imbedded a size-resolved particle growth model, into the gas-phase model to track the temporal evolution of the particle size distribution. The model is initialized with wind speed and size-dependent particle emission and deposition rates and runs to a steady state size distribution prior to initiating monoterpene sea-to-air flux (Text S1). Wind speed-dependent sea spray aerosol particle emission rates are treated using the *Clarke et al.* [2006] parameterization adjusted to the shape of the nascent sea spray aerosol size distribution measured by *Prather et al.* [2013]. Wind speed-dependent particle deposition rates are treated using the parameterization of *Slinn and Slinn* [1980]. Brownian coagulation is included in the model but has a negligible effect on the shape of the particle size distribution over the model sampling period. Following model spin-up, we initiate monoterpene sea-to-air emission to probe the change in the particle size distribution resulting from condensation of ELVOC to the primary aerosol distribution. For maximum monoterpene emission rates (1.1×10^9 molecules cm^{-2} s^{-1}) and Y_{ELVOC} (0.05), and the oxidation and meteorological conditions described for Figure 4, the geometric mean diameter shifted from 175 nm to 200 nm over 48 h. The activation diameter (d_{act}) for sea spray at 0.1% supersaturation is computed assuming a mean particle hygroscopicity parameter (κ) of 0.9 [*Quinn et al.*, 2014; *Schill et al.*, 2015]. If we assume that κ does not change significantly upon vapor deposition of ELVOC, the total number of CCN active particles at 0.1% supersaturation (taken as the integral of the number distribution greater than d_{act}) increases substantially. The percent change in N_{CCN} as a function of N_p and the sea-to-air flux of monoterpenes is shown in Figure 4b. As expected, the percent change in N_{CCN} is most substantial at low N_p and high monoterpene flux, where P_{SOA} is greatest and the SOA produced is distributed onto a smaller number of particles, resulting in a larger shift in the size distribution. For the mean

monoterpene emission rate observed here and very low particle number concentrations (N_p = 50 cm^{-3}), it is expected that N_{CCN} will change by less than 5% over 48 h. For the maximum monoterpene emission rates observed during HiWinGS, N_{CCN} may increase by as much as 20% over 48 h. In contrast, if we assume that ELVOC has a low κ value ($\ll$0.1), there is an insignificant impact of monoterpene oxidation on N_{CCN} as the increase in particle diameter does not accompany a substantial increase in moles of solute and the increase in dry diameter does not significantly impact the Kelvin term of the Köhler equation [*Farmer et al*., 2015].

Recent studies have focused on the role that ELVOC (or highly oxidized organic material) may play in particle nucleation events in pristine locations. While particle nucleation is not explicitly considered here, our model provides context for expected ELVOC concentrations in the North Atlantic. Mean monoterpene sea-to-air emission fluxes (2.63 × 10^7 molecules cm^{-2} s^{-1}) found in this study translate to a steady state monoterpene mixing ratio of less than 5 ppt and ELVOC concentrations less than 5 × 10^5 molecules cm^{-3}. Following *Kirkby et al.* [2016], these concentrations correspond to organic-driven nucleation rates of particles 1.7 nm in diameter ($J_{1.7}$) of less than 10^{-3} cm^{-3} s^{-1}. The peak monoterpene emission rates (1.1 × 10^9 molecules cm^{-2} s^{-1}) observed in this study correspond to steady state monoterpene mixing ratio of approximately 15 ppt and ELVOC concentrations of nearly 3.0 × 10^6 molecules cm^{-3}, for the oxidant and boundary layer conditions described here. Under these rare events, $J_{1.7}$ values could reach 0.002–0.1 cm^{-3} s^{-1} (with the range reflecting differences in neutral versus ion-induced nucleation rates). If these nuclei survive coagulation [*Riipinen et al*., 2012], there is potential for monoterpene ocean emissions to induce new particle formation events.

Acknowledgments

This work was supported by a National Science Foundation (NSF) CAREER Award (grant AGS-1151430). The authors thank the entire High Wind Gas Exchange Study science team. Special thanks go to the WHOI Marine Operations staff, Captain Kent Sheasley, and the capable crew of the R/V *Knorr*. The authors thank the NERC Earth Observation Data Acquisition and Analysis Service (NEODAAS) for supplying refined MODIS chlorophyll *a* data for this study. DMS, isoprene, and monoterpene mixing ratio and vertical flux measurements during HiWinGS are available at https://minds.wisconsin.edu/.

References

Arnold, S. R., et al. (2009), Evaluation of the global oceanic isoprene source and its impacts on marine organic carbon aerosol, *Atmos. Chem. Phys.*, *9*(4), 1253–1262.

Bariteau, L., D. Helmig, C. W. Fairall, J. E. Hare, J. Hueber, and E. K. Lang (2010), Determination of oceanic ozone deposition by ship-borne eddy covariance flux measurements, *Atmos. Meas. Tech.*, *3*(2), 441–455.

Berndt, T., et al. (2016), Hydroxyl radical-induced formation of highly oxidized organic compounds, *Nat. Commun.*, *7*, 13677, doi:10.1038/ncomms13677.

Bertram, T. H., J. R. Kimmel, T. A. Crisp, O. S. Ryder, R. L. N. Yatavelli, J. A. Thornton, M. J. Cubison, M. Gonin, and D. R. Worsnop (2011), A field-deployable, chemical ionization time-of-flight mass spectrometer, *Atmos. Meas. Tech.*, *4*(7), 1471–1479, doi:10.5194/amt-4-1471-2011.

Blomquist, B. W., C. W. Fairall, B. J. Huebert, D. J. Kieber, and G. R. Westby (2006), DMS sea-air transfer velocity: Direct measurements by eddy covariance and parameterization based on the NOAA/COARE gas transfer model, *Geophys. Res. Lett.*, *33*, L07601, doi:10.1029/2006GL025735.

Blomquist, B. W., B. J. Huebert, C. W. Fairall, and I. C. Faloona (2010), Determining the sea-air flux of dimethyl sulfide by eddy correlation using mass spectrometry, *Atmos. Meas. Tech.*, *3*(1), 1–20.

Booge, D., C. A. Marandino, C. Schlundt, P. I. Palmer, M. Schlundt, E. L. Atlas, A. Bracher, E. S. Saltzman, and D. W. R. Wallace (2016), Can simple models predict large-scale surface ocean isoprene concentrations?, *Atmos. Chem. Phys.*, *16*(18), 11,807–11,821, doi:10.5194/acp-16-11807-2016.

Broadgate, W. J., P. S. Liss, and S. A. Penkett (1997), Seasonal emissions of isoprene and other reactive hydrocarbon gases from the ocean, *Geophys. Res. Lett.*, *24*(21), 2675–2678, doi:10.1029/97GL02736.

Broadgate, W. J., G. Malin, F. C. Kupper, A. Thompson, and P. S. Liss (2004), Isoprene and other non-methane hydrocarbons from seaweeds: A source of reactive hydrocarbons to the atmosphere, *Mar. Chem.*, *88*(1–2), 61–73, doi:10.1016/j.marchem.2004.03.002.

Carlton, A. G., C. Wiedinmyer, and J. H. Kroll (2009), A review of secondary organic aerosol (SOA) formation from isoprene, *Atmos. Chem. Phys.*, *9*(14), 4987–5005.

Charlson, R. J., J. E. Lovelock, M. O. Andreae, and S. G. Warren (1987), Oceanic phytoplankton, atmospheric sulfur, cloud albedo and climate, *Nature*, *326*(6114), 655–661, doi:10.1038/326655a0.

Charlson, R. J., J. E. Lovelock, M. O. Andreae, and S. G. Warren (1989), Sulfate aerosols and climate, *Nature*, *340*(6233), 437–438, doi:10.1038/340437a0.

Ciuraru, R., L. Fine, M. van Pinxteren, B. D'Anna, H. Herrmann, and C. George (2015), Unravelling new processes at interfaces: Photochemical isoprene production at the sea surface, *Environ. Sci. Technol.*, *49*(22), 13,199–13,205, doi:10.1021/acs.est.5b02388.

Clarke, A. D., S. R. Owens, and J. C. Zhou (2006), An ultrafine sea-salt flux from breaking waves: Implications for cloud condensation nuclei in the remote marine atmosphere, *J. Geophys. Res.*, *111*, D06202, doi:10.1029/2005JD006565.

Donahue, N. M., and R. G. Prinn (1990), Nonmethane hydrocarbon chemistry in the remote marine boundary layer, *J. Geophys. Res.*, *95*(D11), 18,387–18,411, doi:10.1029/JD095iD11p18387.

Ehn, M., et al. (2014), A large source of low-volatility secondary organic aerosol, *Nature*, *506*(7489), 476–479, doi:10.1038/nature13032.

Farmer, D. K., C. D. Cappa, and S. M. Kreidenweis (2015), Atmospheric processes and their controlling influence on cloud condensation nuclei activity, *Chem. Rev.*, *115*(10), 4199–4217, doi:10.1021/cr5006292.

Fragoso, G. M., A. J. Poulton, I. M. Yashayaev, E. J. H. Head, and D. A. Purdie (2016), Spring phytoplankton communities of the Labrador Sea (2005–2014): Pigment signatures, photophysiology and elemental ratios, *Biogeosci. Discuss.*, *2016*, 1–43, doi:10.5194/bg-2016-295.

Gantt, B., N. Meskhidze, Y. Zhang, and J. Xu (2010), The effect of marine isoprene emissions on secondary organic aerosol and ozone formation in the coastal United States, *Atmos. Environ.*, *44*(1), 115–121, doi:10.1016/j.atmosenv.2009.08.027.

Griffin, R. J., D. R. Cocker, J. H. Seinfeld, and D. Dabdub (1999), Estimate of global atmospheric organic aerosol from oxidation of biogenic hydrocarbons, *Geophys. Res. Lett.*, *26*(17), 2721–2724, doi:10.1029/1999GL900476.

Guenther, A., T. Karl, P. Harley, C. Wiedinmyer, P. I. Palmer, and C. Geron (2006), Estimates of global terrestrial isoprene emissions using MEGAN (Model of Emissions of Gases and Aerosols from Nature), *Atmos. Chem. Phys.*, *6*, 3181–3210.
Hoffmann, T., J. R. Odum, F. Bowman, D. Collins, D. Klockow, R. C. Flagan, and J. H. Seinfeld (1997), Formation of organic aerosols from the oxidation of biogenic hydrocarbons, *J. Atmos. Chem.*, *26*(2), 189–222, doi:10.1023/A:1005734301837.
Houweling, S., F. Dentener, and J. Lelieveld (1998), The impact of nonmethane hydrocarbon compounds on tropospheric photochemistry, *J. Geophys. Res.*, *103*(D9), 10,673–10,696, doi:10.1029/97JD03582.
Hu, Q. H., Z. Q. Xie, X. M. Wang, H. Kang, Q. F. He, and P. F. Zhang (2013), Secondary organic aerosols over oceans via oxidation of isoprene and monoterpenes from Arctic to Antarctic, *Sci. Rep.*, *3*, 2280, doi:10.1038/srep02280.
Johnson, M. T. (2010), A numerical scheme to calculate temperature and salinity dependent air-water transfer velocities for any gas, *Ocean Sci.*, *6*(4), 913–932, doi:10.5194/os-6-913-2010.
Jokinen, T., et al. (2015), Production of extremely low volatile organic compounds from biogenic emissions: Measured yields and atmospheric implications, *Proc. Natl. Acad. Sci. U.S.A.*, *112*(23), 7123–7128, doi:10.1073/pnas.1423977112.
Kawai, H., S. Yabu, Y. Hagihara, T. Koshiro, and H. Okamoto (2015), Characteristics of the cloud top heights of marine boundary layer clouds and the frequency of marine fog over mid-latitudes, *J. Meteorol. Soc. Jpn.*, *93*(6), 613–628, doi:10.2151/jmsj.2015-045.
Kim, M. J., M. C. Zoerb, N. R. Campbell, K. J. Zimmermann, B. W. Blomquist, B. J. Huebert, and T. H. Bertram (2016), Revisiting benzene cluster cations for the chemical ionization of dimethyl sulfide and select volatile organic compounds, *Atmos. Meas. Tech.*, *9*(4), 1473–1484, doi:10.5194/amt-9-1473-2016.
Kirkby, J., et al. (2016), Ion-induced nucleation of pure biogenic particles, *Nature*, *533*(7604), 521–526, doi:10.1038/nature17953.
Kloster, S., J. Feichter, E. M. Reimer, K. D. Six, P. Stier, and P. Wetzel (2006), DMS cycle in the marine ocean-atmosphere system—A global model study, *Biogeosciences*, *3*(1), 29–51.
Kruger, O., and H. Grassl (2011), Southern Ocean phytoplankton increases cloud albedo and reduces precipitation, *Geophys. Res. Lett.*, *38*, L08809, doi:10.1029/2011GL047116.
Lana, A., et al. (2011), An updated climatology of surface dimethlysulfide concentrations and emission fluxes in the global ocean, *Global Biogeochem. Cycles*, *25*, GB1004, doi:10.1029/2010GB003850.
Land, P. E., J. D. Shutler, T. G. Bell, and M. Yang (2014), Exploiting satellite Earth observation to quantify current global oceanic DMS flux and its future climate sensitivity, *J. Geophys. Res. Oceans*, *119*, 7725–7740, doi:10.1002/2014JC010104.
Liu, J., et al. (2016), Efficient isoprene secondary organic aerosol formation from a non-IEPOX pathway, *Environ. Sci. Technol.*, *50*(18), 9872–9880, doi:10.1021/acs.est.6b01872.
Luo, G., and F. Yu (2010), A numerical evaluation of global oceanic emissions of alpha-pinene and isoprene, *Atmos. Chem. Phys.*, *10*(4), 2007–2015.
Matsunaga, S., M. Mochida, T. Saito, and K. Kawamura (2002), In situ measurement of isoprene in the marine air and surface seawater from the western North Pacific, *Atmos. Environ.*, *36*(39–40), 6051–6057, doi:10.1016/S1352-2310(02)00657-X.
McGillis, W. R., J. B. Edson, J. E. Hare, and C. W. Fairall (2001), Direct covariance air-sea CO_2 fluxes, *J. Geophys. Res.*, *106*(C8), 16729–16745.
Meskhidze, N., B. Gantt, and D. Kamykowski (2009), A new physically-based quantification of marine isoprene and primary organic aerosol emissions, *Atmos. Chem. Phys.*, *9*(14), 4915–4927.
Meskhidze, N., and A. Nenes (2006), Phytoplankton and cloudiness in the Southern Ocean, *Science*, *314*(5804), 1419–1423, doi:10.1126/science.1131779.
Meskhidze, N., A. Sabolis, R. Reed, and D. Kamykowski (2015), Quantifying environmental stress-induced emissions of algal isoprene and monoterpenes using laboratory measurements, *Biogeosciences*, *12*(3), 637–651, doi:10.5194/bg-12-637-2015.
Mihalopoulos, N., E. Liakakou, M. Vrekoussis, B. Bonsang, C. Donousis, and M. Kanakidou (2007), Isoprene above the Eastern Mediterranean: Seasonal variation and contribution to the oxidation capacity of the atmosphere, *Atmos. Environ.*, *41*(5), 1002–1010, doi:10.1016/j.atmosenv.2006.09.034.
Nightingale, P. D., G. Malin, C. S. Law, A. J. Watson, P. S. Liss, M. I. Liddicoat, J. Boutin, and R. C. Upstill-Goddard (2000), In situ evaluation of air-sea gas exchange parameterizations using novel conservative and volatile tracers, *Global Biogeochem. Cycles*, *14*(1), 373–387, doi:10.1029/1999GB900091.
Palmer, P. I., and S. L. Shaw (2005), Quantifying global marine isoprene fluxes using MODIS chlorophyll observations, *Geophys. Res. Lett.*, *32*, L09805, doi:10.1029/2005GL022592.
Prather, K. A., et al. (2013), Bringing the ocean into the laboratory to probe the chemical complexity of sea spray aerosol, *Proc. Natl. Acad. Sci. U.S.A.*, *110*(19), 7550–7555, doi:10.1073/pnas.1300262110.
Quinn, P. K., and T. S. Bates (2011), The case against climate regulation via oceanic phytoplankton sulphur emissions, *Nature*, *480*(7375), 51–56, doi:10.1038/nature10580.
Quinn, P. K., T. S. Bates, K. S. Schulz, D. J. Coffman, A. A. Frossard, L. M. Russell, W. C. Keene, and D. J. Kieber (2014), Contribution of sea surface carbon pool to organic matter enrichment in sea spray aerosol, *Nat. Geosci.*, *7*(3), 228–232, doi:10.1038/Ngeo2092.
Riipinen, I., T. Yli-Juuti, J. R. Pierce, T. Petaja, D. R. Worsnop, M. Kulmala, and N. M. Donahue (2012), The contribution of organics to atmospheric nanoparticle growth, *Nat. Geosci.*, *5*(7), 453–458, doi:10.1038/ngeo1499.
Russell, L. M., L. N. Hawkins, A. A. Frossard, P. K. Quinn, and T. S. Bates (2010), Carbohydrate-like composition of submicron atmospheric particles and their production from ocean bubble bursting, *Proc. Natl. Acad. Sci. U.S.A.*, *107*(15), 6652–6657, doi:10.1073/pnas.0908905107.
Schill, S. R., et al. (2015), The impact of aerosol particle mixing state on the hygroscopicity of sea spray aerosol, *ACS Cent. Sci.*, *1*(3), 132–141, doi:10.1021/acscentsci.5b00174.
Shaw, S. L., B. Gantt, and N. Meskhidze (2010), Production and emissions of marine isoprene and monoterpenes: A review, *Adv. Meteorol.*, *2010*, 408696, doi:10.1155/2010/408696.
Slinn, S. A., and W. G. N. Slinn (1980), Predictions for particle deposition on natural waters, *Atmos. Environ.*, *14*(9), 1013–1016, doi:10.1016/0004-6981(80)90032-3.
Spirig, C., A. Neftel, C. Ammann, J. Dommen, W. Grabmer, A. Thielmann, A. Schaub, J. Beauchamp, A. Wisthaler, and A. Hansel (2005), Eddy covariance flux measurements of biogenic VOCs during ECHO 2003 using proton transfer reaction mass spectrometry, *Atmos. Chem. Phys.*, *5*, 465–481.
Stein, A. F., R. R. Draxler, G. D. Rolph, B. J. B. Stunder, M. D. Cohen, and F. Ngan (2015), NOAA's HYSPLIT atmospheric transport and dispersion modeling system, *Bull. Am. Meteorol. Soc.*, *96*(12), 2059–2077, doi:10.1175/Bams-D-14-00110.1.
Taraborrelli, D., M. G. Lawrence, J. N. Crowley, T. J. Dillon, S. Gromov, C. B. M. Gross, L. Vereecken, and J. Lelieveld (2012), Hydroxyl radical buffered by isoprene oxidation over tropical forests (vol 5, pg 190, 2012), *Nat. Geosci.*, *5*(4), 300–300, doi:10.1038/Ngeo1433.

Yang, M. X., B. W. Blomquist, and P. D. Nightingale (2014), Air-sea exchange of methanol and acetone during HiWinGS: Estimation of air phase, water phase gas transfer velocities, *J. Geophys. Res. Oceans*, *119*, 7308–7323, doi:10.1002/2014JC010227.

Yassaa, N., I. Peeken, E. Zollner, K. Bluhm, S. Arnold, D. Spracklen, and J. Williams (2008), Evidence for marine production of monoterpenes, *Environ. Chem.*, *5*(6), 391–401, doi:10.1071/En08047.

Zindler, C., C. A. Marandino, H. W. Bange, F. Schutte, and E. S. Saltzman (2014), Nutrient availability determines dimethyl sulfide and isoprene distribution in the eastern Atlantic Ocean, *Geophys. Res. Lett.*, *41*, 3181–3188, doi:10.1002/2014GL059547.